Mechanism of Integrin Activation by Disulfide Bond Reduction†

Boxu Yan and Jeffrey W. Smith*

Program on Cell Adhesion, The Cancer Research Center, The Burnham Institute, 10901 North Torrey Pines Road, La Jolla, California 92037

Received December 21, 2000; Revised Manuscript Received March 28, 2001

ABSTRACT: Integrin αIIbβ3 plays a pivotal role in hemostasis and thrombosis by mediating platelet adhesion and platelet aggregation. Integrin αIIbβ3 contains an on/off switch that regulates its ligand binding affinity. The switch from "off" to "on" is commonly referred to as integrin activation. We recently identified a redox site within the extracellular domain of the platelet integrin αIIbβ3 that exhibits many properties that one might expect of the on/off switch [Yan, B., and Smith, J. W. (2000) *J. Biol. Chem. 275*, 39964−39972]. Several independent reports show that reducing agents, such as dithiothreitol, can activate integrins. The objective of the present study was to determine if the effects of DTT can be attributed to a perturbation at the integrin redox site. Indeed, we find that DTT reduces two disulfide bonds within the integrin's cysteine-rich domain. Such bond reduction leads to global conformational changes within both αIIb and β3 and the opening of the RGD and fibrinogen binding sites. These findings causally link the reduction of disulfide bonds within the integrin's redox site to transitions in the integrin's activation state.

Integrins are transmembrane receptors that mediate cell adhesion and cell migration (*2*, *3*). The integrin protein family is directly involved in most cell−matrix contacts and cell adhesion events. Many pathologic events, including tumor progression, angiogenesis, and vascular disease, also involve integrins (*4*−*6*). Cell adhesion is tightly regulated by a process called integrin "activation". Activation uncovers the integrin ligand binding site, increasing its ligand binding affinity. The activation and deactivation of integrins is crucial to events such as morphogenesis, tumor cell invasion, and platelet aggregation (*7*−*9*), which is why comprehension of the process, and eventually control and manipulation of its activation, is so crucial.

The subject of this study is platelet αIIbβ3, an integrin whose physiologic function is intimately linked to the process of activation (*9*, *10*). Integrin αIIbβ3 is maintained in a resting state on circulating platelets, but it becomes activated when platelets encounter agonists such as ADP or thrombin. Activation of αIIbβ3 promotes its binding to soluble Fg,[1] and this interaction leads to the formation of a platelet aggregate that halts blood loss. Consequently, activation of αIIbβ3 is key for normal hemostasis. Importantly, though, platelet aggregates can form in pathophysiologic circumstances, such as the rupture of atherosclerotic plaque. In such cases, the platelet aggregate can slow or stop blood flow, causing myocardial infarct (*11*). Therefore, discovering what activates αIIbβ3 could lead to new ways of treating vascular disease.

Many investigators use model systems to study the mechanisms behind integrin activation. For example, studies show that changes in the type or concentration of divalent ions in the extracellular media induce transitions in integrin affinity state (*12*−*14*). Others study transitions in the integrin affinity state by using recombinant integrins in which cytoplasmic domains of either the α subunit or β subunit have been mutated (*15*, *16*). Generating monoclonal antibodies that induce transitions to the affinity state of integrins is another approach (*17*). Finally, treatment of cells with the reducing agent DTT reportedly increases the ligand binding affinity of integrins (*12*, *18*−*20*). Despite the widespread use of each of these methods for modeling integrin activation, we still do not completely understand the mechanism by which they open the ligand binding site(s). Such information is vital if we are to learn how closely the model systems approximate true activation.

In our laboratory, we are defining the conformational distinctions between two purified conformers of the platelet integrin αIIbβ3. The resting conformer is called activation state-1 (AS-1), and the active conformer is called activation state-2 (AS-2). AS-1 and AS-2 have measurably different ligand binding properties. AS-1 is unable to bind to Fg in physiologic Ca^{2+}, and even though it has a functional RGD binding site, this site can only be accessed with RGD peptides linked to affinity columns with extended chemical spacers. In contrast, AS-2 binds rapidly to Fg and has a shallow RGD binding site that is accessible to most RGD peptides. Because the biochemical distinctions between AS-1 and AS-2 are entirely consistent with the changes that take place within αIIbβ3 during activation on whole platelets, we are employing them to distinguish between resting and active integrin.

We recently reported that αIIbβ3 contains a redox site comprised of several unpaired cysteine residues (*1*). This finding raises the question about whether redox modulation could regulate integrin activation and whether one of the

† This study was supported by NIH Grants HL 58925 and CA 69036 to J.W.S., Cancer Center Support Grant CA 30199, and a postdoctoral fellowship from the Western States Affiliate of the AHA to B.Y.

* Corresponding author. Phone: (858)-646-3121. Fax: (858)-646-3192. E-mail: jsmith@burnham.org.

[1] Abbreviations: DTT, dithiothreitol; Fg, fibrinogen; AS-1, activation state-1; AS-2, activation state-2; biotin-BMCC, 1-biotinamido-4-[4′-(maleimidomethyl)cyclohexanecarboximido]butane.

10.1021/bi002902i CCC: $20.00
Published on Web 07/06/2001

models of integrin activation, treatment with DTT, recapitulates the steps in physiologic activation. With the present study, we hope to gain an understanding of the chemical, conformational, and functional changes that take place within AS-1 when it is treated with DTT. In this context, we also sought to clarify the relationship between DTT-induced changes and the known distinctions between AS-1 and AS-2.

EXPERIMENTAL PROCEDURES

Proteins. The two conformers of the αIIbβ3 integrin, AS-1 and AS-2, were purified from outdated human platelets as previously described (*21*−*23*). AS-1 is the resting conformer of the integrin that fails to bind to RGD affinity columns. AS-2 is the activated conformer that is able to bind to RGD affinity resins. Human Fg was purchased from Enzyme Research Laboratories. PAC-1 antibody was the generous gift of Dr. Sandy Shattil, The Scripps Research Institute. V8, AspN-protease, and trypsin (modified sequencing grade) were purchased from Roche Diagnostics Corp.

Reduction of αIIbβ3 with DTT. Purified AS-1 (100 μg) in 100 μL of buffer A (20 mM Tris-HCl, pH 7.4, 150 mM NaCl, 1 mM $CaCl_2$, 1 mM $MgCl_2$, 0.1% Triton X-100) was chilled to 4 °C. DTT was added to a final concentration of 3 mM. Incubation time with DTT varied as noted in the text. Following incubation with DTT, the sample was dialyzed against three changes of buffer A at 4 °C to remove excess DTT.

Measurement of RGD Binding Function with Affinity Resins. To measure the RGD binding function of integrin, the peptide KYGRGDS was coupled to CNBr−Sepharose (Pharmacia Biotech) according to the manufacturer's specifications. AS-1, DTT-treated AS-1, and AS-2 were tested for the ability to bind the resin by incubating 10 μg of each conformer with 20 μL of RGD−Sepharose at 4 °C for 18 h. Then the affinity resin was washed five times with 1 mL of buffer A, and bound integrin was eluted by addition of 20 μL of SDS sample buffer. The eluate was analyzed by SDS−PAGE.

Surface Plasmon Resonance (SPR). The association rate constant, k_1, between Fg and each conformer of αIIbβ3 was measured by SPR using a BIACore 3000. Fg was coupled to the biosensor chip with the amine coupling kit, and the binding to different forms of αIIbβ3 was measured as a function of time. All binding studies were performed in buffer containing 1 mM Ca^{2+} using methods we have previously described (*24*, *25*).

Quantification of Unpaired Cysteine Residues with [^{14}C]Iodoacetamide. To quantify the free cysteines within AS-1, DTT−AS-1, and AS-2, known amounts of each conformer were alkylated with [^{14}C]iodoacetamide. Integrin was denatured by 6 M guanidine hydrochloride, treated with 0.2 M EDTA, and labeled with [^{14}C]iodoacetamide (1:500 molar ratio). The alkylated integrin was quantitatively precipitated with trichloracetic acid, and the pellet was washed several times with Tris buffer (50 mM Tris-HCl, pH 7.4, 100 mM NaCl). The final pellet was resuspended in 10% SDS at 50 °C and then subjected to scintillation counting to determine the incorporation of isotope into integrin.

Modification of αIIbβ3 with Biotin-BMCC. In some experiments the unpaired cysteines within αIIbβ3 were tagged using the sulfhydryl modification reagent 1-biotinamido-4-[4′-(maleimidomethyl)cyclohexanecarboximido] butane (Pierce), using procedures similar to those we have already described (*1*). Briefly, the DTT-treated AS-1 was modified with 0.1 mM biotin-BMCC at ambient temperature for 60 min, followed by dialysis against buffer A at 4 °C for 18 h.

Peptide Mapping. Peptide mapping studies were performed to compare conformational differences between AS-1 and DTT-treated AS-1. V8 protease was added to small samples of the DTT-treated AS-1 or to native AS-1 at a ratio of 1:200 (w/w). Proteolysis was allowed to occur at ambient temperature for 4 h. The reaction was stopped by the addition of SDS sample buffer and heating to 100 °C.

Identification of Fragments of Integrin Containing Free Cysteines. To identify the region of β3 containing free cysteines after treatment with DTT, the reduced integrin was modified with biotin-BMCC as described above and then dialyzed against 4 L of 20 mM NH_4HCO_3 at 4 °C for 18 h. The biotin-tagged sample was digested with V8 protease at a ratio of 1:200 (w/w) at 37 °C for 2 h. To identify peptide fragments that were conjugated to biotin-BMCC, one-half of the sample was incubated with avidin−agarose (Sigma) at 4 °C for 18 h to precipitate the biotin-tagged material. The supernatant of the precipitated digest was then compared to an equivalent amount of the starting material on SDS−PAGE.

Peptide Mass Fingerprinting. To identify the position of peptides within the known sequence of integrin, in-gel tryptic digests were performed as follows: V8 digests of αIIbβ3 were separated on 12% SDS−PAGE under nonreducing conditions. After visualization by silver staining, fragments of interest were excised, digested, and applied to the MALDI target, using procedures we previously reported (*26*). Peptide masses were determined using MALDI-TOF MS on a Voyager DE-RP MALDI-TOF mass spectrometer (PerSeptive Biosystems).

RESULTS

Effect of DTT on the Ligand Binding Function of AS-1. We sought to define the minimal reducing conditions that induce the ligand binding function of purified AS-1. The integrin was treated with 3 mM DTT on ice for either 5 or 45 min. Samples were immediately subjected to dialysis to remove excess DTT. Following dialysis, the samples were analyzed on SDS−PAGE to assess for changes in mobility (Figure 1, lanes 1−4) and were also examined for their ability to bind to KYGRGDS−Sepharose (Figure 1, lanes 5−8). Reduction for 5 min had no discernible effect on the migration of integrin on acrylamide gels (compare lanes 1 and 2) but did sufficiently expose the RGD binding site (compare lanes 5 and 6). More extensive reduction also enhanced the RGD binding function of AS-1 (lane 7), but a reduction of the bond between the heavy chain and the light chain of αIIβ also occurred, as well as changes to the mobility of the β3 subunit.

Integrin αIIbβ3 contains two ligand binding sites, one site for RGD and a separate site for Fg (*24*). AS-2 binds rapidly to Fg in buffer containing Ca^{2+} (*23*). In contrast, AS-1 fails to bind Fg with any appreciable affinity. Given this distinction, we used surface plasmon resonance to determine

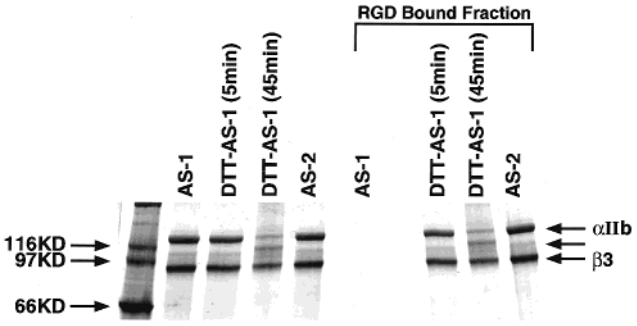

FIGURE 1: DTT activates the RGD binding function of AS-1. The effects of DTT on the mobility (lanes 1−4) and the RGD binding function (lanes 5−8) of AS-1 were tested. Purified AS-1 (lanes 1 and 5) was treated with 3 mM DTT for either 5 min (lanes 2 and 6) or 45 min (lanes 3 and 7) at 4 °C. Samples were then immediately dialyzed against buffer A. Purified AS-2 is shown for comparison (lanes 4 and 8). Following dialysis, samples were analyzed on a nonreducing SDS−PAGE gel (lanes 1−4) or allowed to bind to an affinity column of KYGRGDS−Sepharose. The affinity resin was washed extensively with buffer A to remove unbound integrin, and the bound material was eluted and analyzed by nonreducing SDS−PAGE (lanes 5−8). This experiment was repeated three times, with each repetition yielding similar results.

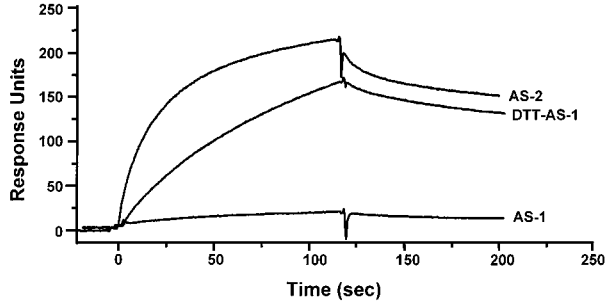

FIGURE 2: DTT increases the association between AS-1 and fibrinogen. The binding of AS-2, AS-1, and AS-1 treated with 3 mM DTT to Fg was measured with SPR using a BIACore 3000. Samples of purified integrin (20 nM) were injected onto a sensor chip conjugated to Fg. Binding was measured in buffer containing 1 mM Ca^{2+}. The resulting sensorgrams are shown. This experiment is one of three repetitions, each yielding nearly identical results.

whether DTT induces the Fg binding function of AS-1. As shown in Figure 2, AS-2, but not AS-1, bound rapidly to Fg. Interestingly, though, DTT-treated AS-1 could bind Fg, albeit at a rate that is about 4-fold slower than AS-2 (3×10^4 vs 1.2×10^5 M^{-1} s^{-1}). This observation indicates that DTT treatment of AS-1 also partially opens the Fg binding site. In support of these observations, we have also observed that DTT will expose the PAC-1 binding site of AS-1 (data not shown).

Effect of Mild Reduction on the Disulfide Bond Status of αIIbβ3. The number of cysteine residues reduced by DTT treatment was determined by alkylating the integrin with [^{14}C]iodoacetamide under strong denaturing conditions. The mole ratio of [^{14}C]iodoacetamide to integrin was measured by scintillation counting. Three independent measurements were made on DTT-treated AS-1, native AS-1, and AS-2 for comparison. As shown in Table 1, DTT-treated AS-1 contains an average of six to seven free cysteine residues. On the basis of this value, we conclude that treatment with DTT causes the reduction of two disulfide bonds in AS-1. Importantly, DTT−AS-1 contains two more free cysteines than AS-2, indicating that the two conformers are chemically distinct.

Table 1: Quantification of the Free Cysteine Residues in AS-1, DTT−AS-1, and AS-2[a]

	no. of free cysteine residues		
repetition	AS-1	DTT−AS-1	AS-2
1	2.7	6.0	4.7
2	2.9	6.8	5.0
3	1.9	7.0	5.2
mean	2.5 ± 0.5	6.6 ± 0.5	4.9 ± 0.2

The free cysteine residues in each form of αIIbβ3 were quantified by measuring the alkylation of the fully denatured integrin with [^{14}C]iodoacetamide as described under Experimental Procedures. Following incorporation of [^{14}C]iodoacetamide, the sample was precipitated with trichloracetic acid and subjected to scintillation counting. The mole ratio of [^{14}C]iodoacetamide incorporated into integrin was then derived from the specific activity of the [^{14}C]iodoacetamide and from the known concentration of integrin used in the alkylation procedure.

Localization of Free Cysteine Residues in DTT-Treated AS-1. We sought to determine if DTT acts within the cysteine-rich domain where the redox site is located (*1*) or if DTT affects disulfides in other regions of the receptor by tagging free cysteine residues within integrin with biotin-BMCC. Ideally, proteolytic fragments of integrin containing the biotin tag would be purified and identified. However, we have been unable to isolate biotin-tagged fragments by affinity purification because of the high binding affinity between avidin and biotin. Therefore, we adopted a biochemical "subtraction" to identify biotin-tagged fragments from DTT-treated AS-1.

DTT-treated AS-1 was modified with biotin-BMCC and then digested with V8 protease. One-half of this digest was applied to avidin−agarose to remove any peptide fragments tagged with biotin-BMCC. The starting material (Figure 3A, lane 1) was compared to the flow-through (Figure 3A, lane 2) on SDS−PAGE. A single band with an approximate mass of 28 kDa (arrow) was precipitated from the digest by avidin−agarose. We cannot exclude the possibility that this procedure also depletes much smaller biotin-tagged fragments, which are not evident because they migrate off of the acrylamide gel. However, we took precautions to ensure only limited digestion of the integrin, so we view this possibility as remote.

The identity of the 28 kDa fragment was determined by peptide mass fingerprinting (Figure 3B). All of the tryptic peptides derived from integrin in this spectrum come from the cysteine-rich domain of β3 (Figure 3C), indicating that the tagged cysteines are confined to this region. Within this mass spectrum, there are two peaks of special importance. The first has a mass of 919 Da, which corresponds to the tryptic peptide extending from residues one to eight in β3, which includes Cys-5. The association of this peptide with the cysteine-rich domain shows that the known long-range disulfide bond between Cys-5 and Cys-435 remains intact upon mild reduction with DTT. The peak with a mass of 1534 Da is also of interest. This is the expected mass of the tryptic peptide extending from β3 residues 490−498, if it were conjugated to biotin-BMCC, indicating that this cysteine is likely to be tagged with biotin-BMCC (see Discussion).

Charting Conformational Changes within αIIbβ3 Induced by DTT. The three conformers of αIIbβ3 appear to exist in

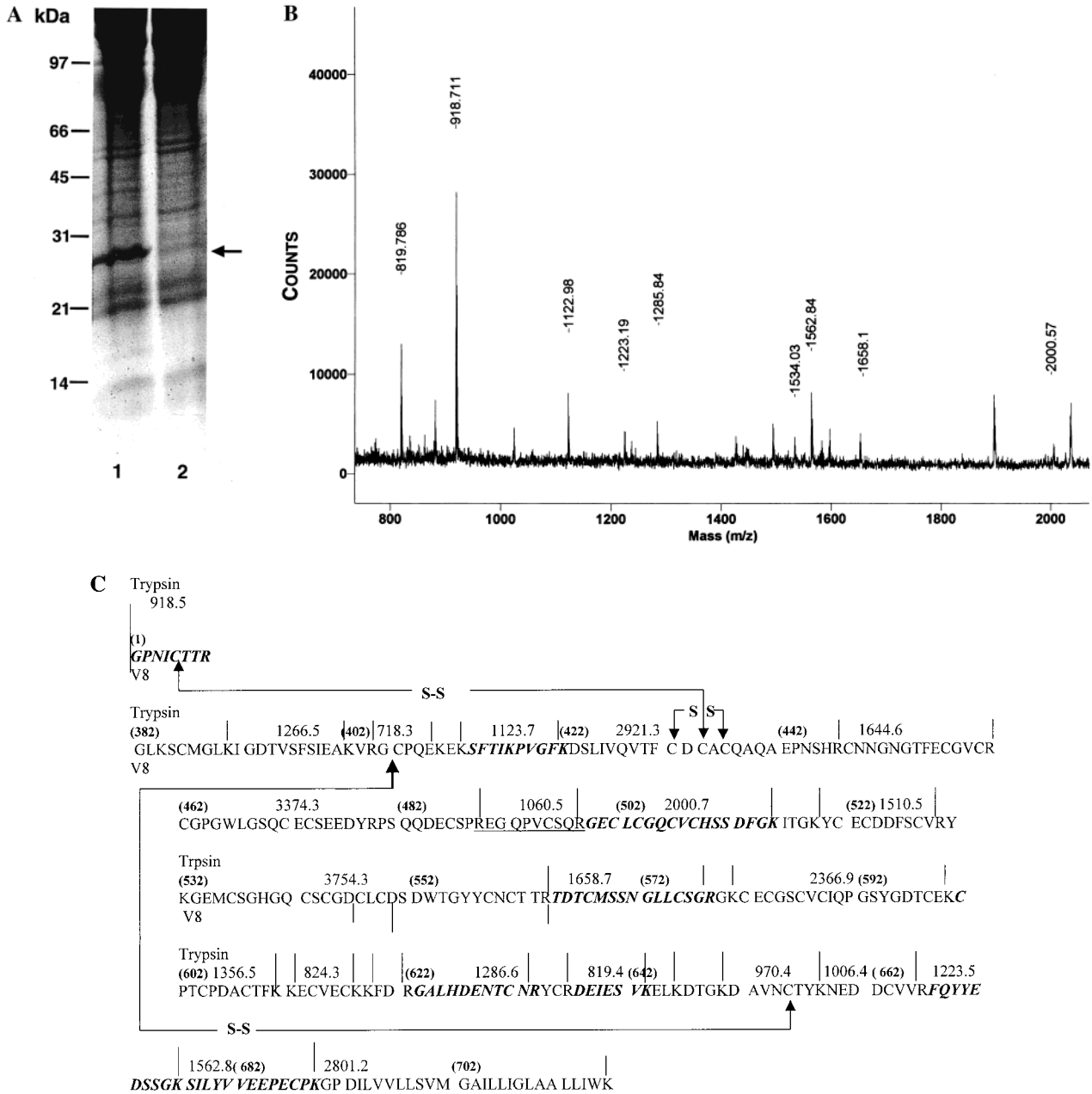

FIGURE 3: Localization of free cysteines in DTT-treated AS-1. (A) AS-1 was treated with 3 mM DTT for 5 min on ice, and then free cysteine residues were modified with biotin-BMCC. The sample was digested with V8 protease as described under Experimental Procedures. Proteolytic fragments containing biotin-BMCC-modified cysteines were identified by determining which peptides could be removed from the digest by avidin−agarose. One-half of the digest was incubated with avidin−agarose for 18 h at 4 °C. This depleted material (lane 2) was compared to the whole digest (lane 1) on SDS−PAGE. Incubation of the digest with avidin−agarose removed a single band with a mass of 28 kDa from the sample (arrow). (B) The composition of the 28 kDa band from lane 1, panel A, was determined by subjecting the excised band to in-gel tryptic digestion followed by peptide mass fingerprinting with MALDI-TOF MS. The *m*/*z* profile of this sample within the range of 800−2200 Da is shown. All of the peptides derived from the β3 subunit are labeled above the peak with their exact mass. One additional peak, with a mass of 1534, is also labeled as it may correspond to a peptide comprised of β3 residues 490−498 linked to biotin-BMCC. (C) The amino acid sequence of the cysteine-rich domain of β3 is shown in order to illustrate the position of the peptides detected in MALDI-TOF (panel B). Two known long-range disulfide bonds are shown with arrows. Predicted tryptic and V8 cleavage points are noted with lines above the sequence. The mass of each predicted fragment is also shown. Eight peptides (bold text) from this domain are detected in the MALDI profile (panel B). The tryptic fragment with a mass of 1060.5 (underlined) may be tagged with biotin-BMCC because a peak with an appropriate mass (1534 Da) is observed in the MALDI spectra.

stable but distinct conformations. We conducted experiments to probe the relationship between these conformers. By exposing each to a range of DTT concentrations for 15 min, we measured their sensitivity to reduction. The mobility of the reduced integrins was compared on acrylamide gels under nonreducing conditions. Each conformer showed a different sensitivity to reduction. AS-1 undergoes a major conformational transition at 2.5 mM DTT (Figure 4A, arrow). In contrast, DTT−AS-1 is affected by much lower concentrations of DTT. The αIIβ3 subunit is fully reduced by the lowest concentration of DTT, and the β3 subunit undergoes conformational transitions at 0.5 mM DTT (Figure 4B,

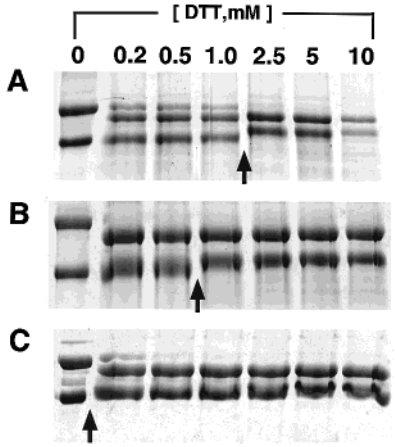

FIGURE 4: Effect of DTT on the microenvironment of disulfide bonds of integrin αIIbβ3. The effect of DTT on the disulfide bonds within AS-1 (A), DTT−AS-1 (B), and AS-2 (C) was measured using gel electrophoresis. Each conformer was incubated with a range of DTT concentrations (noted at top of figure) for 3 min on ice. The reaction was quenched by addition of 50 mM reduced glutathione. Samples were analyzed on 7.5% acrylamide gels and visualized by Coomassie Blue staining.

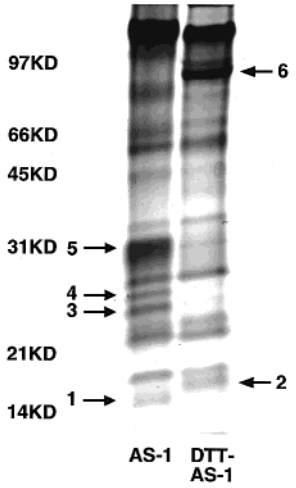

FIGURE 5: Conformational changes induced by DTT are revealed by peptide mapping. Peptide mapping studies were performed to identify regions of integrin that exhibit conformational changes as a result of treatment with DTT. AS-1 (lane 1, left) and DTT-treated AS-1 (lane 2, right) were digested with V8 protease at a ratio of 1:200 (protease:αIIbβ3 w/w) at 37 °C overnight. The resulting peptide fragments were separated on 11% SDS−PAGE under nonreducing conditions and then visualized by staining with Coomassie Blue. Several bands unique to either AS-1 or DTT-treated AS-1 are labeled (arrows 1−6).

arrow). AS-2 is the most sensitive to DTT, with all mobility shifts occurring at the lowest concentration of DTT (Figure 4C).

Mapping Conformational Differences with Limited Proteolysis. Peptide mapping was also used to assess the similarity between DTT−AS-1, native AS-1, and AS-2. Initial peptide maps showed DTT−AS-1 and AS-2 to have substantially different conformations (data not shown). In contrast, native AS-1 and DTT−AS-1 appeared to be closely related. An in-depth analysis with V8 protease revealed some important distinctions between these two conformers (Figure 5). V8 fragments that differed in the two peptide maps were subjected to mass fingerprinting so that the positions of distinction could be mapped within the known sequence of integrin.

Because DTT reduces bonds within the cysteine-rich domain, one might expect to observe conformational changes in this region of the integrin. Indeed, fragment 5 (lane 1, arrow), which is present only in the V8 digest of AS-1, is derived from this domain. Mass fingerprinting shows this fragment to contain β3 residues 393−422 and 490−716 (see Table 1 in Supporting Information). These two regions are connected by a disulfide bond between Cys-406 and Cys-655 and encompass major portions of the cysteine-rich domain.

Fragments 1 (from AS-1) and 2 (from DTT−AS-1) differ in mass on SDS−PAGE but are both derived from the N-terminal portion of β3. This region contains the N-terminal disulfide knot linked to a major portion of the I-like domain that comprises the ligand binding site (*27*). Interestingly, peptides with masses of 1171.7 and 1532.5 Da are present in fragment 2 (DTT−AS-1) but are absent in the mass fingerprints of fragment 1 (see Table 2 in Supporting Information). These two tryptic fragments correspond to residues 63−72 and 73−78, which make up a linker between the N-terminal knot and the I-like domain.

Conformational changes induced by DTT are not limited to the β3 subunit. Fragment 6, an 80 kDa fragment unique to the V8 digest of DTT−AS-1, also contains the cation binding sites of αIIb (mass fingerprint not shown). This band is absent from the digest of native AS-1, where the cation binding sites of αIIb are found split among fragments 3 and 4. Results from mass fingerprinting of these V8-generated peptides are shown in Table 3 of Supporting Information.

DISCUSSION

A number of studies have shown that physiologic redox agents such as nitric oxide (NO) and *S*-nitrosothiols (*28*, *29*), along with *S*-nitrosoalbumin (*30*), have potent inhibitory effects on platelet adhesion and aggregation. There is also evidence that mice lacking platelet NO synthase have enhanced hemostatic capability (*31*) and that patients with impaired production of platelet NO have a higher risk of acute coronary syndromes (*32*). The mechanism by which these redox agents influence the vasculature is only partially understood.

Our recent observation that integrins display a redox site comprised of unpaired cysteines (*1*) indicates that a direct effect of redox agents on integrins must be considered. This idea is supported by the recent finding that platelet protein disulfide isomerase can regulate ligand binding by αIIbβ3 (*33*). When coupled with prior reports showing that treatment of cells with DTT can increase an integrin's ligand binding affinity (*12*, *18*−*20*), these observations strongly suggest that oxidation−reduction reactions within integrin could be of mechanistic significance. With these ideas in mind, the primary objective of this study was to understand the mechanism by which mild reduction increases the ligand binding affinity of the resting form of αIIbβ3.

Mild reducing conditions are sufficient to convert AS-1 to an active conformer. The RGD and Fg binding properties of the resting integrin can be stimulated by treating the integrin with 3 mM DTT for only 5 min on ice. This renders the RGD binding site accessible to peptide affinity columns

and also exposes the Fg binding site. It should be emphasized that reduction with DTT is the only treatment we have identified that converts AS-1 to a stable conformer capable of binding Fg in Ca^{2+}. A systematic search of a number of different salts and chaotropic agents failed to identify any condition that could elicit this conformational change in AS-1 (D. Hu and J. Smith, unpublished observations). Even the divalent ion Mn^{2+}, which increases the ligand binding affinity of AS-1, is unable to elicit a conformational change that is stable and could be considered activation. When Mn^{2+}-treated AS-1 is dialyzed back into Ca^{2+}, it loses its ability to bind to Fg (*23*). Hence, the effects of DTT on AS-1 appear to be unique.

Importantly, the exposure of the Fg binding site by DTT appears to be incomplete. The association rate between DTT−AS-1 and Fg remains approximately 4-fold slower than the rate at which AS-2 binds to Fg (3×10^4 vs 1.2×10^5 M^{-1} s^{-1}). Consequently, mild reduction appears to only partially activate AS-1. This finding is in agreement with prior work showing that DTT supports slower platelet aggregation and the formation of smaller than normal aggregates (*18*).

The mechanism by which DTT promotes the ligand binding function of AS-1 appears to lie in its ability to reduce select disulfide bonds. Mild reduction of AS-1 increased the number of unpaired cysteine residues from two to approximately six, an increase equating to the reduction of only two disulfide bonds. Although the effect of DTT on ligand binding affinity of integrins is well-known, this is the first demonstration, of which we are aware, showing that the effects of DTT are actually at the level of disulfide bond reduction. A prior report focusing on the β2 integrins concluded that mild reduction was without effect of the integrin's disulfide bonds (*19*), a finding that should probably be reevaluated on the basis of results presented here.

Bonds that are reduced by DTT appear to be confined to the cysteine-rich domain of β3. We observed only a single 28 kDa fragment that could be depleted from proteolytic digests of biotin-BMCC-modified DTT−AS-1 using avidin−agarose affinity resin. By use of tryptic mass fingerprinting, this fragment was found to encompass the major portion of the cysteine-rich domain. An identical analysis of native AS-1 that was also tagged with biotin-BMCC failed to identify any fragment. In fact, our inability to capture a biotin-BMCC-tagged fragment of native AS-1 led to our use of reversible sulfhydryl modification reagents to identify the domain that displays free cysteines (*1*). The ability to capture, or at least deplete, tagged fragments of DTT−AS-1 probably demonstrates the fact that DTT partially unfolds the integrin, exposing the tagged sulfhydryls so that they are better able to bind to the shallow biotin binding pocket on avidin.

All integrin β subunits contain 56 conserved cysteine residues. Two of these are commonly referred to as "long-range" bonds because they link residues that are distant in the primary sequence. These long-range disulfides link Cys-5 with Cys-435 and Cys-406 to Cys 655 (*27*). Although one might anticipate DTT to reduce these long-range disulfide bonds in the integrin, we are able to exclude the disulfide bond between Cys-5 and Cys-435 as a target for DTT. This bond remains intact in V8-generated fragments obtained from DTT−AS-1. The other long-range disulfide bond, between Cys 406 and Cys-655, remains a potential target for DTT.

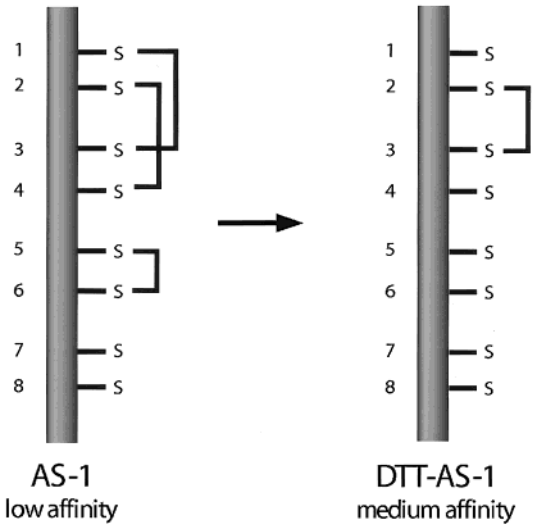

FIGURE 6: Model of the redox transitions induced by DTT. The results of the present study show that mild reduction of AS-1 with DTT causes an overall net reduction of two disulfide bonds. Our prior work reported that modification of the free sulfhydryls in AS-1 with biotin-BMCC prevented activation of the integrin by DTT (*1*). In conjunction with the present findings, this would indicate that, along with a net reduction, DTT also induces a disulfide bond rearrangement. In the model, AS-1 is depicted using a hypothetical ensemble of eight cysteine residues, which form three disulfides and present two free sulfhydryls. DTT-induced reduction and rearrangement are illustrated by the acquisition of a new disulfide bond between cysteines 2 and 3 and the corresponding loss of disulfides between cysteines 1 and 3, 2 and 4, and 5 and 6.

In fact, this bond is a likely candidate because a prior study shows that its reduction places integrin into an active conformation (*34*). Both Cys-406 and Cys-655 are within the domain of DTT−AS-1 that we identified as containing the free sulfhydryls (Figure 3C).

Another bond that is a likely target for DTT is the bond that connects Cys-457 with Cys-495. We observed a peak with a mass of 1534 Da in the tryptic digest of biotin-BMCC-tagged DTT−AS-1. This peak corresponds to the exact mass of a tryptic peptide extending from residue 490 to residue 498, provided it were tagged with biotin-BMCC. Within this peptide there is a single cysteine, Cys-495, which was unequivocally identified in a disulfide bond with Cys-457 in a prior study (*27*). The presence of this peak, the absence of any peak corresponding to the iodoacetamide adduct of this tryptic peptide, and the knowledge that Cys-495 exists in a disulfide bond all argue strongly that this cysteine is one of the targets of DTT. This disulfide bond connects the first and second cysteine-rich repeats within β3.

The present study leads to a working model of the cysteine residues that comprise the redox site (Figure 6). This model takes into account our prior work on the redox site (*1*) and another recent observation showing that αIIbβ3 exhibits enzymatic protein−disulfide isomerase activity (*35*). The redox site in resting integrin is depicted as a hypothetical ensemble of eight cysteine residues, two of which remain unpaired. As shown here, reduction with DTT leads to an overall net reduction of two of the disulfides within this ensemble. Importantly, though, the effects of DTT are more complicated than simple bond reduction. Our prior work showed that modification of the free cysteines within AS-1 with biotin-BMCC could block DTT-induced activation (*1*). Consequently, the free cysteines that are unpaired in native

AS-1 are required for the transitions in affinity state induced by DTT. This requirement could be explained by a disulfide bond rearrangement that involves the originally unpaired cysteines, along with an overall bond reduction. Such a rearrangement is consistent with the fact that αIIbβ3 exhibits the enzymatic ability to catalyze disulfide bond rearrangements (*35*). This model can now be used as a framework to interpret future work aimed at understanding the rearrangements of the redox site during physiologic and pathophysiologic transitions in affinity state.

SUPPORTING INFORMATION AVAILABLE

Three tables giving mass fingerprinting of V8-generated fragments and peptides. This material is available free of charge via the Internet at http://pubs.acs.org.

REFERENCES

1. Yan, B., and Smith, J. W. (2000) *J. Biol. Chem. 275*, 39964−39972.
2. Ruoslahti, E. (1996) *Annu. Rev. Cell Dev. Biol. 12*, 697−715.
3. Hynes, R. O. (1992) *Cell 69*, 11−25.
4. Ruoslahti, E., and Giancotti, F. G. (1989) *Cancer Cells 1*, 119−126.
5. Varner, J. A., and Cheresh, D. A. (1996) *Curr. Opin. Cell Biol. 8*, 724−730.
6. Coller, B. S., Anderson, K., and Weisman, H. F. (1995) *Thromb. Haemostasis 74*, 302−308.
7. Martin-Bermudo, M. D., Dunin-Borkowski, O. M., and Brown, N. H. (1998) *J. Cell Biol. 141*, 1073−1081.
8. Palecek, S. P., Loftus, J. C., Ginsberg, M. H., Lauffenburger, D. A., and Horwitz, A. F. (1997) *Nature 385*, 537−540.
9. Marguerie, G. A., Edgington, T. S., and Plow, E. F. (1980) *J. Biol. Chem. 255*, 154−161.
10. Phillips, D. R., Charo, I. F., and Scarborough, R. M. (1991) *Cell 65*, 359−362.
11. Jang, Y., Lincoff, A. M., Plow, E. F., and Topol, E. J. (1994) *J. Am. Coll. Cardiol. 24*, 1591−1601.
12. Ni, H., Li, A., Simonsen, N., and Wilkins, J. A. (1998) *J. Biol. Chem. 273*, 7981−7987.
13. Masumoto, A., and Hemler, M. E. (1993) *J. Biol. Chem. 268*, 228−234.
14. Dransfield, I., Cabanas, C., Craig, A., and Hogg, N. (1992) *J. Cell Biol. 116*, 219−226.
15. O'Toole, T. E., Katagiri, Y., Faull, R. J., Peter, K., Tamura, R., Quaranta, V., Loftus, J. C., Shattil, S. J., and Ginsberg, M. H. (1994) *J. Cell Biol. 124*, 1047−1059.
16. Vinogradova, O., Haas, T., Plow, E. F., and Qin, J. (2000) *Proc. Natl. Acad. Sci. U.S.A. 97*, 1450−1455.
17. Frelinger, A. L., III, Du, X. P., Plow, E. F., and Ginsberg, M. H. (1991) *J. Biol. Chem. 266*, 17106−17111.
18. Peerschke, E. I. (1995) *Thromb. Haemostasis 73*, 862−867.
19. Edwards, B. S., Curry, M. S., Southon, E. A., Chong, A. S., and Graf, L. H., Jr. (1995) *Blood 86*, 2288−2301.
20. Edwards, B. S., Southon, E. A., Curry, M. S., Salazar, F., Gale, J. M., Robinson, M. K., Graf, L. H., Jr., and Born, J. L. (1998) *J. Leukocyte Biol. 63*, 190−202.
21. Fitzgerald, L. A., Leung, B., and Phillips, D. R. (1985) *Anal. Biochem. 151*, 169−177.
22. Kouns, W. C., Hadvary, P., and Steiner, B. (1992) *J. Biol. Chem. 267*, 18844−18851.
23. Yan, B., Hu, D. D., Knowles, S. K., and Smith, J. W. (2000) *J. Biol. Chem. 275*, 7249−7260.
24. Hu, D. D., White, C. A., Panzer-Knodle, S., Page, J. D., Nicholson, N., and Smith, J. W. (1999) *J. Biol. Chem. 274*, 4633−4639.
25. Hu, D. D., Barbas, C. F. I., and Smith, J. W. (1996) *J. Biol. Chem. 271*, 21745−21751.
26. Landry, F., Lombardo, C. R., and Smith, J. W. (2000) *Anal. Biochem. 279*, 1−8.
27. Calvete, J. J., Henschen, A., and Gonzalez-Rodriguez, J. (1991) *Biochem. J. 274*, 63−71.
28. Simon, D. I., Stamler, J. S., Jaraki, O., Keaney, J. F., Osborne, J. A., Francis, S. A., Singel, D. J., and Loscalzo, J. (1993) *Arterioscler. Thromb. 13*, 791−799.
29. Mendelsohn, M. E., O'Neill, S., George, D., and Loscalzo, J. (1990) *J. Biol. Chem. 265*, 19028−19034.
30. Keaney, J. F., Jr., Simon, D. I., Stamler, J. S., Jaraki, O., Scharfstein, J., Vita, J. A., and Loscalzo, J. (1993) *J. Clin. Invest. 91*, 1582−1589.
31. Freedman, J. E., Sauter, R., Battinelli, E. M., Ault, K., Knowles, C., Huang, P. L., and Loscalzo, J. (1999) *Circ. Res. 84*, 1416−1421.
32. Freedman, J. E., Ting, B., Hankin, B., Loscalzo, J., Keaney, J. F., Jr., and Vita, J. A. (1998) *Circulation 98*, 1481−1486.
33. Lahav, J., Gofer-Dadosh, N., Luboshitz, J., Hess, O., and Shaklai, M. (2000) *FEBS Lett. 475*, 89−92.
34. Liu, C. Y., Sun, Q. H., Wang, R., Paddock, C. M., and Newman, P. J. (1997) *Blood 90*, 573a.
35. O'Neill, S., Robinson, A., Deering, A., Ryan, M., Fitzgerald, D. J., and Moran, N. (2000) *J. Biol. Chem. 275*, 36984−36990.

BI002902I